

Fast Ultrasound Image Simulation using the Westervelt Equation

Athanasios Karamalis¹, Wolfgang Wein² *, and Nassir Navab¹

¹ Computer Aided Medical Procedures, Technische Universität München, Germany
karamali@cs.tum.edu

² White Lion Technologies AG, Munich, Germany

Abstract. The simulation of ultrasound wave propagation is of high interest in fields as ultrasound system development and therapeutic ultrasound. From a computational point of view the requirements for realistic simulations are immense with processing time reaching even an entire day. In this work we present a framework for fast ultrasound image simulation covering the imaging pipeline from the initial pulse transmission to the final image formation. The propagation of ultrasound waves is modeled with the Westervelt equation, which is solved explicitly with a Finite Difference scheme. Solving this scheme in parallel on the Graphics Processing Unit allows us to simulate realistic ultrasound images in a short time.

Key words: Ultrasound Simulation, Westervelt Equation, Finite Difference Method, GPU

1 Introduction

The realistic simulation of medical ultrasound has applications in fields such as ultrasound system development. Here the quality of ultrasound images depends highly on numerous system parameters including for example transducer shape, focusing strategies and active aperture size. To speed up prototyping and lower development costs engineers simulate the effects of different system parameterizations before moving on to the actual system assembly [6]. A more recent application domain is the simulation of High Intensity Focused Ultrasound (HIFU), also referred to as Therapeutic Ultrasound. The nonlinear propagation of ultrasound in tissue produces high-frequency components that are absorbed more rapidly by the tissue. Simulating these effects is crucial for the correct assessment of the ultrasound dose required for therapy and is subject to ongoing research [2]. In terms of education, the physics and instrumentation of ultrasound are complex and require in-depth knowledge to understand the impact of different system parameterizations on the final image [15]. A fast simulation can demonstrate the results of different system parameterizations and provide more insights into the underlying mechanisms of the imaging modality. Last but

* Work conducted while at Siemens Corporate Research, Princeton, NJ, USA

not least, ultrasound simulation has recently been utilized for multimodal image registration between CT and ultrasound [13]. A similarity measure is evaluated between the real ultrasound images and ones simulated from CT. Improving the simulation could also improve the accuracy and robustness of the registration.

The overall processing time is a decisive factor for the simulation of ultrasound. Simulating a single ultrasound scan line using the Westervelt equation and a Finite Difference scheme was reported to take about 1 hour on a desktop PC [5], with the simulation of a complete image requiring probably more than a day of processing time. Furthermore, alternative simulation approaches like Field II [6], one of the most widely used linear ultrasound simulation packages, can require up to two days of processing time on a modern desktop PC for generating a single 128 scan line ultrasound image [10].

In Pinton et al. [9] a thorough comparison was presented between the Westervelt equation and alternatively proposed methods for modeling ultrasound wave propagation. They presented simulated ultrasound images by solving the Westervelt equation with a Finite-Difference Time-Domain scheme, whereas, details on the Radio-Frequency (RF) processing for the image formation were omitted.

In this work we focus on the realistic simulation of ultrasound wave propagation and the subsequent generation of ultrasound images in acceptable time. For this purpose the ultrasound imaging pipeline was implemented from the initial pulse transmission to the final image formation. The wave propagation is modeled using the Westervelt equation, which is explicitly solved with a Finite Difference scheme. In order to achieve fast simulation times the Finite Difference scheme was implemented on the Graphics Processing Unit (GPU), which has already demonstrated its potential for accelerating parallel computations and efficiently solving these schemes [3, 8].

2 Wave Propagation

The propagation of ultrasound waves and their interaction with different media was modeled using the Westervelt Partial Differential Equation (PDE), also referred to as the nonlinear full-wave equation [2, 5]. It describes the propagation of waves and additionally models thermal attenuation and nonlinearity. The reader interested in an accuracy analysis of the Westervelt equation is referred to Huijssen et al. [5], which includes comparisons to an analytical solution, the Khokhlov-Zabolotskaya-Kuznetsov equation and water tank measurements. The Westervelt equation is given as follows:

$$\nabla^2 p - \frac{1}{c_0^2} \frac{\partial^2 p}{\partial t^2} + \frac{\delta}{c_0^4} \frac{\partial^3 p}{\partial t^3} + \frac{\beta}{\rho_0 c_0^4} \frac{\partial^2 p^2}{\partial t^2} = 0, \quad (1)$$

where p [Pa] is the acoustic pressure, c_0 [ms^{-1}] is the propagation speed, ρ_0 [kgm^{-3}] is the ambient density, δ [m^2s^{-1}] is the diffusivity of sound, and β is the coefficient of nonlinearity. Thus, the first two terms are identical to the D'Alembertian operator on p , the third term is the loss term due to thermal conduction and the fourth term describes the nonlinearity.

One thing to note is that various simulation approaches model sound waves as rays, taking into account the physics from optics [10, 13]. This simplification results in faster processing times, but reduces significantly the realism of the simulation. Ray based simulation approaches are not able to fully model the complex effects modeled by wave based approaches. These effects include interference, scattering, diffraction etc. which are common in medical ultrasound propagation and contribute tremendously to the formation of the final ultrasound image. For more details on ultrasound image characteristics and artifacts see Zagzebski [15].

The Westervelt equation is numerically solved with the Finite Difference method [1, 3, 8]. The basic idea behind this method is to evaluate the PDE equation, more specifically calculate the wave amplitude, on sampling points of a computational grid. The grid can have complex shapes, while we use a regular 2D grid with equidistant sampling points. For the calculation of the wave amplitude the partial derivatives of the equation are substituted with their finite difference representations and the equation is solved for the future timestep. A thorough analysis of higher order Finite Difference schemes for solving the acoustic wave equation is presented by Cohen and Joly [1]. Fourth-order accurate in space and second-order accurate in time schemes have demonstrated good results [1, 2], and are therefore used in our work. The finite differences for equation (1) are given as follows:

$$\frac{\partial p}{\partial t} \approx \frac{p_{i,j}^n - p_{i,j}^{n-1}}{\Delta t}, \quad \frac{\partial^2 p}{\partial t^2} \approx \frac{p_{i,j}^{n+1} - 2p_{i,j}^n + p_{i,j}^{n-1}}{\Delta t^2}, \quad (2)$$

$$\frac{\partial^3 p}{\partial t^3} \approx \frac{6p_{i,j}^n - 23p_{i,j}^{n-1} + 34p_{i,j}^{n-2} - 24p_{i,j}^{n-3} + 8p_{i,j}^{n-4} - p_{i,j}^{n-5}}{(2\Delta t)^3}, \quad (3)$$

$$\frac{\partial^2 p}{\partial x^2} \approx \frac{-p_{i+2,j}^n + 16p_{i+1,j}^n - 30p_{i,j}^n + 16p_{i-1,j}^n - p_{i-2,j}^n}{12\Delta x^2}, \quad (4)$$

$$\frac{\partial^2 p}{\partial y^2} \approx \frac{-p_{i,j+2}^n + 16p_{i,j+1}^n - 30p_{i,j}^n + 16p_{i,j-1}^n - p_{i,j-2}^n}{12\Delta y^2}, \quad (5)$$

where i, j are the axial and the lateral indices of the discrete computational grid, n is the timestep, $\Delta x, \Delta y$ are the spatial discretization steps and Δt is the temporal discretization step. Thus, an explicit solution is calculated for each sampling point based on the wave amplitudes at sampling points of the previous timesteps.

To model the interaction of the waves with heterogeneous media, different coefficients are used for the speed of sound, the ambient density, the diffusivity of sound and the nonlinearity. The most important effect in ultrasound imaging is the reflection of the waves, which is caused by the difference in speed of sound between media.

3 Ultrasound Image Simulation

In our framework we implemented the basic procedure to synthesize B-mode ultrasound images. Other than the wave propagation, the image simulation pro-

cess involves transmission and reception of ultrasound pulses and processing of the resulting echoes for forming the final image. For more details on ultrasound physics, instrumentation and image formation see Hedrick et al. [4] and Szabo [11].

3.1 Ultrasound Transmission and Reception

For each simulation run sound waves are emitted at selected points on the computational grid. Various transducer geometries can be simulated by selecting the appropriate points on the grid, with a linear transducer modeled in this work. Modifying the wave amplitude at these points introduces a wave disturbance that propagates through the grid with the simulation of consecutive timesteps. The shape of the emitted pulse is of crucial importance. Non-modulated sinusoidal or Gaussian shaped pulses for instance can cause grid disturbances even after the pulse transmission has ceased. We use a 6 cycle sinusoidal pulse modulated by a Gaussian shaped envelope, commonly used by ultrasound systems [4]. The pulse is formulated as follows:

$$s(t) = \left(A \cdot \sin \left(\frac{2\pi}{l} t \right) \right) \left(\alpha e^{-\frac{(x - \mu)^2}{2\sigma^2}} \right), \quad (6)$$

where $s(t)$ is the pulse amplitude at timestep $t \in [0..l]$, l is the pulse length, A is the maximal pulse amplitude, α is the Gaussian amplitude, x is the random variable, μ the mean, and σ is the standard deviation. The echoes are recorded for each timestep at the positions where the grid was perturbed by the pulse transmission. Ultrasound images are formed from multiple scan lines with the total number of scan lines playing an important role for the overall spatial resolution of the final ultrasound image. Each scan line in the ultrasound image corresponds to the echoes received along an ultrasound beam, which brings us to topic of ultrasound beamforming.

Beamforming refers to the constructive/destructive interference of waves emitted by multiple transducer elements. Triggering a group of transducer elements at a time results in high acoustic intensities along the center axis of the group. Figure 1(a) schematically shows the process of focusing using a group of elements and figure 1(b) shows the simulation run, with our framework, for beam focusing at a low depth. Generating a narrow beam is desirable in ultrasound system development as it improves the spatial resolution of the ultrasound scan. Additionally, triggering the transducer with the appropriate time delays allows to position and steer the beam [4].

Multiple scan lines are acquired for the image formation by transmitting a beam, receiving the echoes and moving the active element group until the entire transducer element surface is covered.

3.2 Radio Frequency Processing

The result of the previously described simulation is Radio Frequency (RF) data acquired for each element of an active element group for each scan line. Before forming an image, the raw data needs to be processed. The RF processing

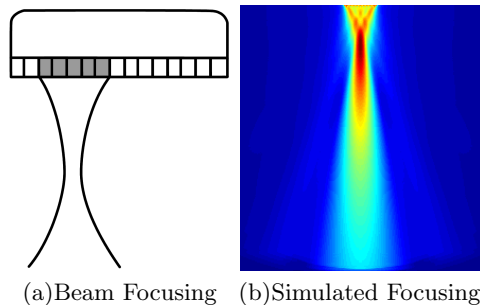


Fig. 1. Image (a) schematically demonstrates ultrasound beam focusing by triggering a group of elements with different time delays. Image (b) shows the maximum wave amplitudes of a simulation run using a focus scheme for low depths in a medium with uniform speed of sound.

pipeline varies slightly between different ultrasound system vendors, but the basic principles are common and are implemented in this framework.

An ultrasound scan line is formed by combining the RF data acquired at each element of an active element group. For this we apply the Delay and Sum beamforming algorithm [12], which can among others be defined as:

$$d(t) = \sum_{i=0}^N W_i \cdot e_i(t + \tau), \quad (7)$$

where $d(t)$ is the final signal response of an ultrasound beam at timestep t , N is the number of active transducer elements, W_i is a weighting function (in our case a Hanning window), $e_i(t)$ is the signal response of each active transducer element i , and τ is the transmission delay expressed in timesteps.

The received signal contains noise that is mainly manifested in the low and high frequency parts of its spectrum [11]. Therefore, the low and high frequency components are removed with a bandpass filter, in our case a Butterworth filter.

Afterwards the signal goes through the process of demodulation, which results in a signal that retains its overall pulse response but contains much less high frequency modulations. Demodulation is performed by finding the envelope of the rectified signal and is implemented by taking the absolute of the Hilbert Transform of the signal.

As a pulse traverses through the medium it is attenuated and reflectors at greater depth appear weaker than reflectors at smaller depth. This is compensated by applying a so-called Time-Gain Compensation (TGC), which amplifies echoes based on their reception time (depth). In our implementation the signal is convolved with a simple linear function $f \in [1..n]$, where n is the amplification factor for the maximal depth.

Last but not least, the resulting signal $h(t)$ is compressed by decreasing its dynamic range (ratio of strongest to weakest signal). This is usually done with

a logarithmic scaling (also referred to as log-compression):

$$h_c(t) = \log(h(t) + c), \quad (8)$$

where c is the compression coefficient. At this point the ultrasound image is formed by combining the processed RF lines into a single image.

4 Results

The proposed simulation framework was utilized for generating 2D ultrasound images out of two synthetic datasets, one showing a fetus, figure 2(a), and the other one showing multiple anechoic regions embedded in a highly scattering medium, figure 2(c). The fetus dataset is a modified version of the one presented in Jensen and Munk [7] and the phantom dataset is generated using Rayleigh noise, with similar phantoms being used for testing real ultrasound imaging systems [4]. The mediums had following characteristics: $\delta = 4.5 \cdot 10^{-6} [m^2 s^{-1}]$, $\beta = 6$ and $\rho_0 = 1100 [kg m^{-3}]$, which are common for human tissue [14].

The corresponding simulated ultrasound images are shown in figure 2(b) and 2(d). They clearly demonstrate a realistic speckle pattern, interference effects and beam focusing artifacts. The spatial resolution is high at the center of the focal zone and decreases with increasing distance from the focal zone, an effect also observed in real ultrasound imaging. Furthermore, interference of echoes is strongly evident in the anechoic regions of the phantom dataset. Following parameters were used for simulating the presented ultrasound images: 11 transducer elements formed the active group, $\lambda/2$ elements spacing was used, 192 scan lines were processed, and the discretization steps were set to $\Delta x = \Delta y = 5 \cdot 10^{-3} [m]$ and $\Delta t = 5.5 \cdot 10^{-7} [s]$. For the fetus dataset 6000 timesteps were evaluated and for the phantom dataset 8600, because of the increased depth.

The simulation of the ultrasound wave propagation for generating the raw RF data is performed on the GPU using C++, OpenGL, and the GL shading language (GLSL). Implementing the Finite Difference scheme on the GPU is relatively straight forward with explicit and implicit solvers presented in Harris [3] and Krüger et al. [8] respectively. Switching from GLSL to C-like GPU programming languages like CUDA or OpenCL might improve the performance since they offer more elaborate shared memory features.

After simulating the scan lines, the resulting RF data is processed on the CPU, as there are no computationally expensive tasks involved. For a 2048^2 grid and 192 scan lines the RF simulation on the GPU required 55 minutes for the fetus dataset and 78 minutes for the phantom dataset, with the image formation on the CPU requiring 19 seconds and 24 seconds respectively. The performance was evaluated on a desktop PC with an Intel Core 2 2.66 GHz with 4 GB RAM and a NVIDIA GeForce GTX 280 with 1GB VRAM. In comparison, the framework presented in Pinton et al. [9] required 32 hours processing time on a 56 PC cluster with 118 GB RAM for a 3D simulation. Details on the processing time of the 2D simulation were omitted, but should be in the same range given the provided parameterizations. Furthermore, one simple 2D image was simulated from a synthetic dataset containing only a single anechoic region.

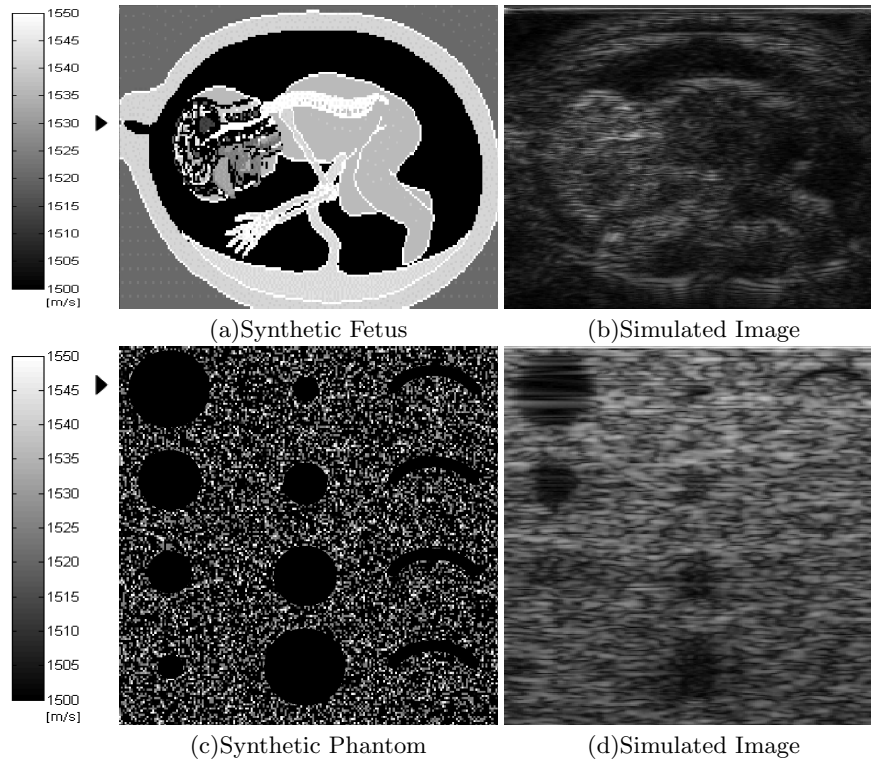


Fig. 2. Image (a) shows the synthetic fetus dataset and image (c) the synthetic phantom dataset. The intensity values correspond to speed of sound values in the range of 1500-1550 [m/s]. The center of the focal zones are marked with a small triangle on the left side. Image (b) and (d) show the simulated ultrasound images.

5 Conclusion

In this work we presented a framework for fast ultrasound image simulation, covering the imaging pipeline from the initial pulse transmission to the final image formation. Our implementation on the GPU simulates realistic ultrasound images in under 80 minutes, avoiding the cumbersome use of PC clusters. The considerably lower simulation time, compared to other implementations, has practical implications for most simulation related application domains like ultrasound system development. Particularly, our approach has strong implications for future intra-operative simulation of HIFU treatment, as the simulation of a single focal zone is computed in less than 30 seconds. Furthermore, simulating on the GPU allows for an interactive visualization of the wave propagation during the simulation at almost no computational cost, which is of interest to both education and system development applications.

In our current implementation the simulation grid is extended to prevent reflections at the grid boundary from interfering with the region of interest in the

simulation grid. Implementing Absorbing Boundary Conditions, similar to [9], could notably improve the overall performance of the simulation as less grid cells would need to be evaluated. This would pave the way for utilizing our framework for 3D ultrasound simulation in acceptable time.

Acknowledgments. We would like to thank Christian Wachinger for valuable discussions. This work was partly funded by the European Project PASSPORT and Siemens Corporate Research, Princeton, NJ, USA.

References

1. Gary Cohen and Patrick Joly. Construction and Analysis of Fourth-Order Finite Difference Schemes for the Acoustic Wave Equation in Nonhomogeneous Media. *SIAM Journal on Numerical Analysis*, 33(4):1266–1302, 1996.
2. I.M. Hallaj and R.O. Cleveland. FDTD Simulation of Finite-Amplitude Pressure and Temperature Fields for Biomedical Ultrasound. *The Journal of the Acoustical Society of America*, 105:7–12, 1999.
3. M. Harris. Fast Fluid Dynamics Simulation on the GPU. *GPU Gems*, 1:637–665, 2004.
4. W.R. Hedrick, D.L. Hykes, and D.E. Starchman. *Ultrasound Physics and Instrumentation*. Mosby, 2005.
5. J. Huijssen, A. Bouakaz, M.D. Verweij, and N. de Jong. Simulations of the Nonlinear Acoustic Pressure Field without using the Parabolic Approximation. In *IEEE Symposium on Ultrasonics*, volume 2, pages 1851–1854, 2003.
6. J.A. Jensen. Field: A Program for Simulating Ultrasound Systems. *Medical and Biological Engineering and Computing*, 34:351–352, 1996.
7. J.A. Jensen and P. Munk. Computer Phantoms for Simulating Ultrasound B-mode and CFM Images. *Acoustical Imaging*, 23(75-80), 1997.
8. J. Krüger and R. Westermann. Linear Algebra Operators for GPU Implementation of Numerical Algorithms. *GPU Gems*, 2, 2005.
9. G.F. Pinton, J. Dahl, S. Rosenzweig, and G.E. Trahey. A Heterogeneous Nonlinear Attenuating Full-Wave Model of Ultrasound. *IEEE Transactions on Ultrasonics, Ferroelectrics, and Frequency Control*, 56:474–488, 2009.
10. R. Shams, R. Hartley, and N. Navab. Real-Time Simulation of Medical Ultrasound from CT Images. In *Medical Image Computing and Computer-Assisted Intervention (MICCAI)*, volume 2, pages 734–741, 2008.
11. T.L. Szabo. *Diagnostic Ultrasound Imaging: Inside Out*. Academic Press, 2004.
12. K.E. Thomenius. Evolution of Ultrasound Beamformers. In *IEEE Ultrasonics Symposium*, pages 1615–1622, 1996.
13. W. Wein, S. Brunke, A. Khamene, M.R. Callstrom, and N. Navab. Automatic CT-Ultrasound Registration for Diagnostic Imaging and Image-Guided Intervention. *Medical Image Analysis*, 12:577–585, 2008.
14. S. Yongchen, D. Yanwu, T. Jie, and T. Zhensheng. Ultrasonic Propagation Parameters in Human Tissues. In *IEEE Ultrasonics Symposium*, pages 905–908, 1986.
15. J.A. Zagzebski. *Essentials of Ultrasound Physics*. Mosby, 1996.